ELSEVIER

Ceramics International 30 (2004) 629–634

CERAMICS INTERNATIONAL

www.elsevier.com/locate/ceramint

Sintering, sinterforging and explosive compaction to densify the dual phase nanocomposite system Y_2O_3-doped ZrO_2 and RuO_2

Tomas P. Raming [a,*], Werner E. van Zyl [a], Erik P. Carton [b], H. Verweij [a,1]

[a] *Laboratory for Inorganic Materials Science, Faculty of Chemical Technology, MESA Research Institute, University of Twente, P.O. Box 217, AE Enschede 7500, The Netherlands*

[b] *TNO Prins Maurits Laboratory, P.O. Box 45, AA Rijswijk 2280, The Netherlands*

Received 2 June 2003; received in revised form 29 June 2003; accepted 2 September 2003

Available online 5 May 2004

Abstract

Yttria-doped zirconia/ruthenia powders were made by co-precipitation. The calcined powders were compacted into green compacts using standard pressing techniques such as isostatical compaction compared to explosive compaction. Explosive compaction (EC) led to the highest density, but also to cracking of the compacts. The zirconia/ruthenia powders compacted by isostatical pressing could not be densified by pressureless sintering (58%), but sinterforging these green compacts led to dense compacts (96%), which showed large-scale phase separation between the yttria-doped zirconia and ruthenia phase. The explosively densified green compacts could be further densified to 92% by pressureless sintering, without the occurrence of the large-scale phase separation that took place within the isostatically pressed (IP) and sinterforged (SF) samples. The microstructure of the explosively densified composites was more fine-grained and homogeneous. Thus, by tuning the green density of yttria-doped zirconia/ruthenia compacts the phase separation after sintering can be tuned. This phase separation largely determines the electrical properties of these materials, which means that these electrical properties will be tunable as well.

Keywords: A. Mixing; A. Powders: chemical preparation; B. Composites; D. ZrO_2

1. Introduction

Zirconia/ruthenia dual-phase composites are thought of mainly as electrode material [1,2]. Ruthenia has a high metallic conduction [3], while zirconia, when doped with yttria, is an oxygen ion-conducting material [4]. Yttrium doped zirconia/ruthenia composites could also have interesting properties such as mixed oxygen-ionic electronic conduction [5,6] and high capacitance. The main reason for adding zirconia to ruthenia, however, has been to increase the stability of ruthenia, when used as a dimensionally stable electrode [1,2]. The addition of zirconia to ruthenia helps to protect the ruthenia against the reactions that takes place above 700 °C where the material becomes volatile as RuO_3 and/or RuO_4 (in oxygen-containing atmospheres) or reduces to Ru^0 (in reducing atmospheres) [7]. Furthermore, the costs of the electrodes are reduced by the addition of zirconia. Provided a percolation path for ruthenia remains, addition of this second phase does not lead to substantial decrease in electron conductivity. Up to 85 mol% of insulating TiO_2 has been added to ruthenia without losing the electron conduction properties [8,9].

The zirconia/ruthenia composites that were reported previously were either porous gels [5,10–13] or porous layered electrodes [1,2,14]. Only recently the synthesis of a dense bulk 3Y-TZP (zirconia doped with 3 mol% yttria, having a tetragonal phase)-ruthenia electrode has been disclosed [15]. This composite was obtained by first making a zirconia/ruthenia powder through a co-precipitation method and subsequently sinterforging (SF) the calcined powder at the relatively low temperature of 1150 °C. Sinterforging (also called hot pressing) was chosen as densification method since sintering without added pressure did not lead to densification of the ruthenia/3Y-TZP materials [15]. Although the resulting compact was dense and hardly had lost any ruthenia during sinterforging, the microstructure showed large-scale phase separation within the compact between the zirconia and ruthenia phases caused by the aforementioned oxidation reaction of ruthenia. This large-scale phase separation, however, led to a high electrical conductivity [15].

* Corresponding author.

[1] Present address: Department of Materials Science and Engineering, The Ohio State University, Columbus, OH 43210-1178, USA.

0272-8842/$30.00
doi:10.1016/j.ceramint.2003.09.006

This large-scale phase separation is not desirable for all possible applications of these composites. If the grains of both phases could be kept small during densification of the ruthenia/3Y-TZP, the material would have a much larger internal grain boundary surface. A more homogeneous microstructure would increase the percolation limit, and thereby the capacitance of non-percolative ruthenia/3Y-TZP systems. The electrical properties thus depend very much on the microstructure of these type of ceramics, much more compared to single phase electroceramics.

The ruthenia grain growth and dehomogenisation during sinterforging was due to the high temperature necessary for the densification. If the densification would occur at lower temperature, this might reduce the ruthenia grain growth and dehomogenisation. To achieve more rapid densification at lower temperatures, in order to suppress this phase separation and ruthenia grain growth process, the 3Y-TZP/ruthenia powders were explosively compacted. This technique has been reported to enable the densification of zirconia powders, up to around 90% density, at relatively low temperatures. By additional sintering these compacts were fully densified [16]. Densification of a ruthenia powder by explosive compaction has been reported to be quite difficult. Large amounts of copper powder were added to function as lubricant, to achieve stronger compacts. Unfortunately no densities were mentioned [17].

The here for the first time reported explosively compacted 3Y-TZP/ruthenia powders were further densified by pressureless sintering. The densification and microstructure of these compacts was compared with the earlier reported sinterforged 3Y-TZP/ruthenia powders [15]. Different green compaction methods were compared. By using explosive compaction and subsequent sintering 92% dense, but cracked specimens could be obtained with a novel, more homogeneous and fine-grained microstructure.

2. Experimental

2.1. Powder synthesis

Powder synthesis has been described before [15]. A powder was prepared through co-precipitation (CP*X*), in which a solution of $ZrOCl_2{\cdot}8H_2O$, YCl_3 and $RuCl_3{\cdot}3.4H_2O$ was added to aqueous ammonia (pH 14) with vigorous stirring, where *X* denotes the molar percentage of RuO_2 present (determined by X-ray fluorescence spectrometry (XRF)) in the powder. The gels were washed with water to remove any water-soluble species and subsequently with ethanol to remove water. After drying at 100 °C the gels were mortared and calcined in air at 600 °C for 2 h with a heating rate of 2 °C/min.

2.2. Green compaction methods

These ruthenia/yttria-doped zirconia composite powders, and also a single-phase yttria-doped zirconia powder, were densified into green compacts, using three different compaction techniques: isostatistical pressing (IP), uniaxial pressing (UP) and explosive compaction (EC).

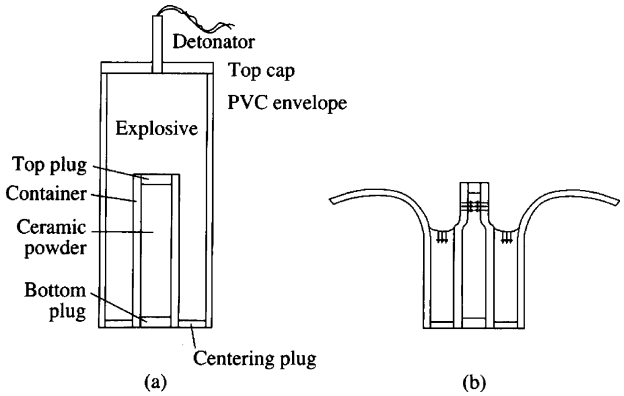

Fig. 1. Set-up used for explosive compaction.

One part of the calcined powder thus was isostatically pressed at 400 MPa, after pre-pressing in a rubber mould at 200 MPa. The isostatic pressing resulted in cylindrical samples with dimensions of ±8 mm length and ±6 mm diameter. A second part was uniaxially pressed at 1000 MPa in a cylindrical steel mould with diameter 10 mm. The resulting compacts had a height of 1–2 mm.

Some powders were also densified by using explosive compaction. A mild steel tube with an inner diameter of 10 mm, a wall thickness of 2.2 mm and a length of 95 mm was used as a powder container. The 3Y-TZP/RuO_2-powder mixture, sandwiched between two layers of pure 3Y-TZP powder, was pre-compacted in the container by uniaxial pressing (UP) to a relative density of 33% of the theoretical density. Both ends of the tube were stoppered by steel plugs. The powder container was centered in a PVC-cylinder with an inner diameter of 60 mm and a length of 150 mm. The remaining space was filled with 450 g of an ammoniumnitrate-based explosive with a detonation velocity of 3.6 km/s; a melange called AMPA [18]. A detonator was placed on top of the cylindrical configuration. The explosive compaction experiment was performed inside a bunker at room temperature. The set-up is shown in Fig. 1a and b gives a schematic representation of the progressing shock wave and the resulting compaction of the inner steel tube with powder.

After the electrical activation of the detonator an axially sliding detonation front ran along the powder container. The high pressure within the detonation wave caused a radially collapsing of the powder container and introduced a converging shock wave in the powder. The pressure within this initial shock wave was of the order of 1 GPa. A second, diverging shock wave occurred upon reflection of the initial shock wave at the axis. The pressure behind the reflected shock wave was several times higher than the pressure in the initial shock wave. At the reflection of the second shock wave at the periphery of the powder container the first rarefaction wave entered the powder as a first step of pressure release [18].

2.3. Sintering

The green compacts that were sinterforged were pre-sintered by heating with 2 °C/min to 800 °C, and kept at this temperature for 2 h before cooling down to room temperature, as described before [15]. The resulting compacts were placed between SiC pistons and sinterforged using the following program:

- Heating with 10 °C/min to 800 °C
- Heating with 2 °C/min up to 50 °C below the set temperature for SF
- Heating further with 2 °C/min up to the set temperature (1150 °C) while increasing the pressure from 0 to the final pressure (100 MPa)
- Keeping the temperature and pressure constant for 25 min
- Relieving the pressure and cooling down to room temperature

The green compacts that were sintered pressureless (PS) were heated with 2 °C/min until the set temperature, kept at the set temperature for 2 h and then cooled down with 4 °C/min back to room temperature.

2.4. Characterisation

The composition of the powders and compacts was determined with quantitative XRF using a Philips PW 1480/10-fluorometer (Eindhoven, The Netherlands). All measurements were done in duplicate. The powders were pressed into a tablet. The X-ray fluorescence spectrometry-measurement method has been described previously [19].

The phase composition of the compacts was investigated with a Philips X'Pert-1 PW3710 X-ray diffraction (XRD) diffractometer (Eindhoven, The Netherlands), using Cu Kα radiation. The divergence slit was set to either 1° using a Ni-filter in the secondary (diffracted) beam or to an irradiated length of 10 mm when using a secondary curved graphite monochromator optimized for Cu-radiation. The receiving slit was set to 0.1 mm in all cases.

The density of the compacts was determined using the Archimedes technique. The used liquid was mercury for non-dense (<90%) compacts and water for dense (>90%) compacts.

The compacts were analysed with scanning electron microscopy (SEM) coupled with an energy dispersive X-ray microanalysis system (EDAX-mapping). A Philips XL30 ESEM-FEG (environmental scanning electron microscope with field emission gun) was used to make BackScatter Electron (BSE) and secondary electron (SE)-micrographs at different magnifications (Eindhoven, The Netherlands). The SEM was coupled with an EDAX DX4 system (resolution 132 eV for Mn Kα) that was used to make electron maps (EDAX, Mahwah, NJ, USA).

3. Results

3.1. Compaction of powders

The molar compositions of the powders, calcined at 600 °C have been determined by quantitative XRF. The results are shown in Table 1 (for an explanation of the names of the compacts: see Section 2.1).

The obtained densities for the three used green compaction techniques (IP, UP and EC) are shown in Table 2. It is clear that the explosive compression technique led to the highest green density, but the resulting compacts showed severe cracking. XRD showed that the phases of the ruthenia and 3Y-TZP had remained unchanged, after the explosive compaction.

Uniaxial pressing at 1000 MPa yielded composite green samples that were not cracked, reaching densities over 60%, although UP1000-CP46 showed some laminar cracks. The 3Y-TZP compact showed severe laminar cracking after uniaxially pressing at 1000 MPa, even if a binder was added to the powder before pressing. Isostatical pressing in all cases resulted in non-cracked samples.

3.2. Sintering behaviour of compacts

The green compacts that were pre-compacted by IP and EC were further densified by sinterforging and pressureless sintering (PS). In Table 3 the densities obtained with these sintering methods using a temperature of 1150 °C are mentioned. The isostatically pressed CP33 powder could only be densified into a dense compact by using sinterforging, while 3Y-TZP was densified without added pressure at 1150 °C. The explosively compacted 3Y-TZP powder could also be densified more easily with pressureless sintering than the explosively compacted CP33 powder, as can be seen in Fig. 2.

Table 1
Quantitative XRF data showing the molar composition of the system Y_2O_3-doped ZrO_2/RuO_2 composite powders after calcination at 600 °C

Powder	ZrO_2 (mol%)	Y_2O_3 (mol%)	HfO_2 (mol%)	RuO_2 (mol%)	Cl (mol%)
CP46	49.7	3.1	0.5	46.3	0.1
CP33	63.0	3.2	0.6	33.0	0.2
CP15	79.4	4.1	1.0	15.1	0.4

Table 2
Relative density of compacts after different powder compaction methods: isostatical pressing (IP), uniaxial pressing (UP) and explosive compaction (EC)

	Press method		
	IP	UP	EC
Relative density (%)			
CP46	58.9	63.1	–
CP33	51.8	60.5	78.4
CP15	54.5	60.4	–

Table 3
Relative density of compacts after different pre-compaction and subsequent sintering methods: isostatical pressing (IP), explosive compaction (EC), pressureless sintering (PS) and sinterforging (SF)

Pre-compaction method	IP	EC	IP
Sinter method	PS	PS	SF
Relative density (%)			
CP33	58	92	96
3Y-TZP	97	97	–

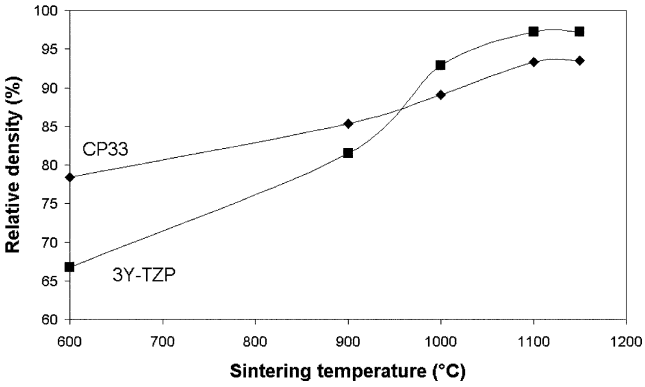

Fig. 2. Relative densities of powder compacts made by explosive compaction after sintering at increasing temperatures for 2 h.

The samples prepared by explosive compaction have been sintered pressureless at increasing temperatures up to 1150 °C with a 2 h hold at each sintering temperature. The increase of density with sintering temperature is shown in Fig. 2. The 3Y-TZP compact had a lower density compared to the CP33 compact after explosive compaction, but obviously a higher sinter-activity, since at 1000 °C the density of the 3Y-TZP compact was already higher.

3.3. The microstructure of the sintered compacts

Fig. 3 shows the microstructure of CP33 sinterforged at 1150 °C under 100 MPa. Segregation between the ruthenia and zirconia phases had occurred on macroscopic scale, as reported before [15]. The ruthenia that was present near the surfaces of the pores between the remainders of the agglomerates sublimed into these pores and subsequently condensed there during the closure of the pores. As a result in the peripheries of the original agglomerates only zirconia remained, causing the darker colouration of these peripheries in Fig. 3, while the pores between them were filled with ruthenia. In the bulk of the original agglomerates a homogenous distribution of small (below 200 nm) ruthenia and zirconia grains was present, as can be seen in Fig. 4.

The microstructure of the explosively compacted CP33 powder that subsequently was sintered (pressureless) at 1150 °C was quite different to the CP33 powder that was sinterforged at 1150 °C. First of all, it showed very large cracks (see Fig. 5), resulting off course from the explosive pre-compaction. These cracks were the major cause for the

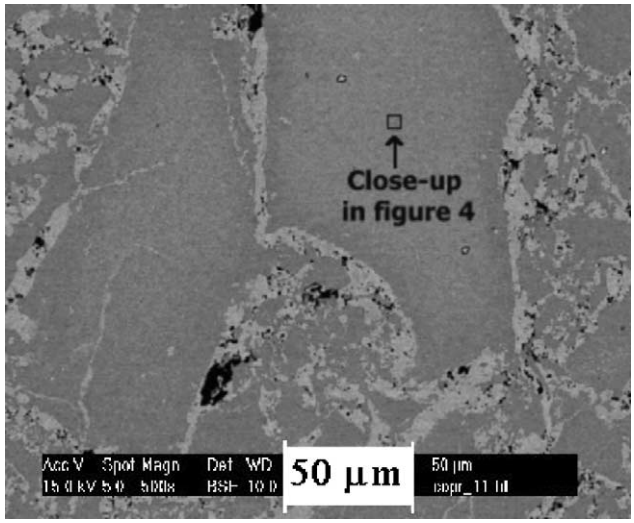

Fig. 3. BSE–SEM picture of CP33 compact sinterforged at 1150 °C at 100 MPa. Light areas are pure RuO_2.

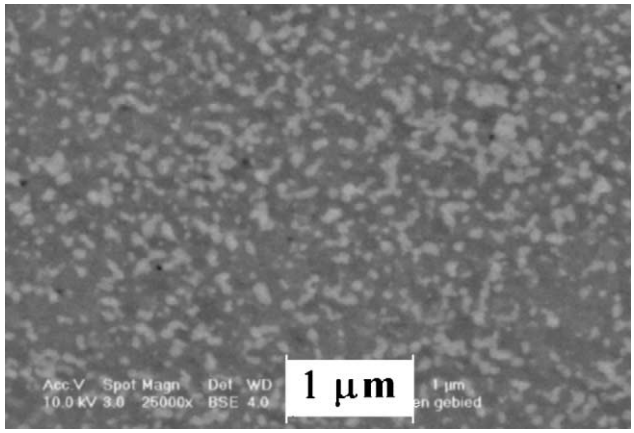

Fig. 4. BSE–SEM picture of bulk area of CP33 compact sinterforged at 1150 °C at 100 MPa. Light areas: ruthenia. Dark areas: zirconia.

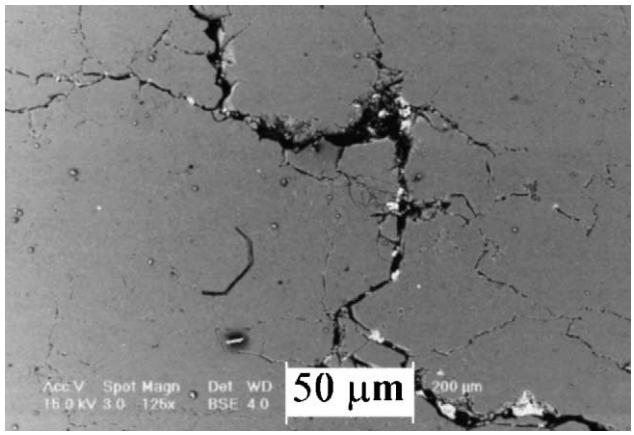

Fig. 5. BSE–SEM picture of explosively compacted CP33 compact after pressureless sintering at 1150 °C.

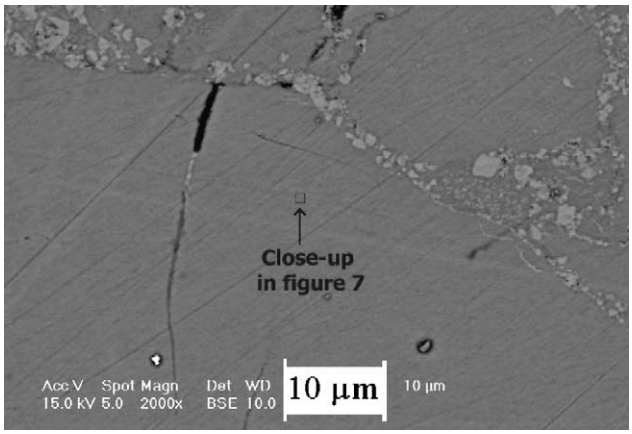

Fig. 6. BSE–SEM picture of explosively compacted CP33 compact after pressureless sintering at 1150 °C. Light areas: ruthenia.

8% porosity of this compact. Isostatic pressing of the powders and subsequent sinterforging did not lead to cracking, but Fig. 3 (and Table 3) do show that the sinterforged CP33 compact had some large pores at the original agglomerate boundaries.

Another major difference between the sinterforged and explosively compacted CP33 zirconia/ruthenia composite was that the explosively compacted CP33 powder that subsequently was sintered (pressureless) at 1150 °C showed much less phase separation between the zirconia and ruthenia phases compared to the sinterforged CP33 compact, as can be seen by comparing Figs. 3 and 6. The SEM-investigation showed the presence of ruthenia grains of maximally 2 μm in or at pores and cracks of the explosively compacted CP33 composite, but the severe drainage of ruthenia from large areas near pores and cracks that had occurred during the sinterforging of the isostatically compressed CP33 composite (as in Fig. 3) had not occurred during the sintering of the explosively compacted composites (compare with Fig. 6). The large majority of the explosively compacted CP33 powder that subsequently was sintered (pressureless) at 1150 °C consisted of a homogeneous distribution of small grains of the two phases (see Fig. 7), as was also present to a lesser extent in the sinterforged CP33 compact (see Fig. 4).

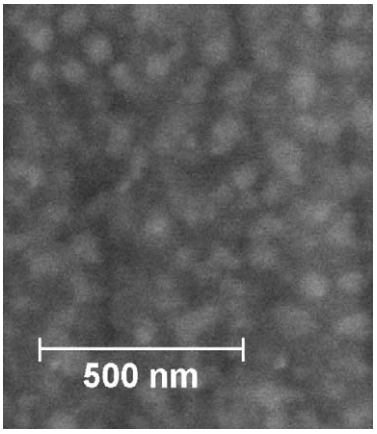

Fig. 7. BSE–SEM picture of the bulk of explosively compacted CP33 compact after pressureless sintering at 1150 °C. Light areas: ruthenia. Dark areas: zirconia.

4. Discussion

The green compaction tests showed that the presence of the relatively soft ruthenia in the mixed 3Y-TZP/RuO_2 powders improved the pressing behaviour compared to the hard single-phase 3Y-TZP powder, higher densities were obtained and less cracking occurred. The ruthenia seems to act as a lubricant. In almost all cases the 3Y-TZP green compact obtained the lowest density.

At the moment sintering starts, the situation changes, however. The presence of ruthenia obstructs the densification of the composites. Single-phase 3Y-TZP densifies more easily than all the 3Y-TZP/ruthenia composites, probably as a result of the oxidation reaction of ruthenia.

The explosive compaction, although resulting in cracked compacts, did lead to a high enough green density for the CP33 compact to severely limit the phase separation during the subsequent sintering step. The phase segregation inside the zirconia/ruthenia compacts during sintering seems to depend strongly on the amount of porosity. With lower porosity less ruthenia is present near a pore and less ruthenia will segregate into these pores. Thus, the amount of segregation between the zirconia and ruthenia phases in a ruthenia/zirconia dual phase compact can be tuned by varying the starting density of the compact to be sintered.

Improvement of the process parameters of the explosive compaction process might lead to non-cracked samples and even higher green densities. Regarding the fact that the zirconia/ruthenia powders can be easily compacted into green compacts by standard pressing techniques, and regarding the fact that alumina–zirconia composites could be densified into non-cracked green compacts with 90% density by explosive compaction [20], this last result might be attainable for zirconia/ruthenia powders as well.

If non-cracked samples would be obtained, they could be probed for their electrical, which might be very interesting. If the system has a percolative path for electric conduction, it might be useful as oxygen ion membrane. When the composite does not have electric conduction, it might have a high capacitance. The more homogeneous microstructure that has been obtained now will have a higher percolation limit that the zirconia/ruthenia system described before [15], which will lead to a higher capacitance for non-percolative systems.

5. Conclusions

A density of 78% was obtained for a dual phase zirconia/ruthenia powder at room temperature by using explosive

compaction. The severely cracked green compact was further densified by pressureless sintering. After pressureless sintering at 1150 °C the explosively compacted powder had a density of 93%, with the large cracks remaining.

Dense (above 95%) dual phase zirconia/composites could be obtained by sinterforging at 1150 °C under 100 MPa pressure starting with 52% dense isostatically pressed green compacts. Sinterforging the zirconia/ruthenia compacts at 1150 °C led to macroscopic phase segregation, while in the case of explosive compaction and subsequent pressureless sintering the phase separation between the two phases was much less. Thus, by varying the density of the zirconia/ruthenia green compacts the amount of phase separation after sintering can be tuned. The higher the green density before sintering, the lower the phase separation after sintering will be.

Acknowledgements

Coen van Dijk of the University of Groningen is acknowledged for making the many SEM-pictures. We gratefully acknowledge the Netherlands Organisation for Scientific Research (NWO), group of Chemical Sciences (CW) for financial support.

References

[1] O.R. Camara, S. Trasatti, Surface electrochemical properties of Ti/(RuO_2 and ZrO_2) electrodes, Electrochim. Acta 41 (1996) 419–427.
[2] L.D. Burke, M. McCarthy, Oxygen gas evolution at, and deterioration of, RuO_2/ZrO_2-coated titanium anodes at elevated temperature in strong base, Electrochim. Acta 29 (1984) 211–216.
[3] J.B. Goodenough, Metallic oxides, Prog. Solid State Chem. 5 (1971) 145–399.
[4] S. Jiang, W.A. Schulze, V.R.W. Amarakoon, G.C. Stangle, Electrical properties of ultrafine-grained yttria-stabilised zirconia ceramics, J. Mater. Res. 12 (1997) 2374–2380.
[5] M.T. Colomer, J.R. Jurado, Preparation and electrical characterisation of ruthenia-doped yttria-stabilised zirconia ceramics, J. Solid State Chem. 141 (1998) 282–289.
[6] M. Hrovat, J. Holc, D. Kolar, Thick film ruthenium oxide/yttria-stabilised zirconia-based cathode material for solid oxide fuel cells, Solid State Ionics 68 (1994) 99–103.
[7] V.K. Tagirov, D.M. Chizhikov, E.K. Kazenas, L.K. Shubochkin, Thermal dissociation of ruthenium dioxide and rhodium sesquioxide, Russ. J. Inorg. Chem. 20 (1975) 1133–1135.
[8] S. Trasatti, Physical electrochemistry of ceramic oxides, Electrochim. Acta 36 (1991) 225–241.
[9] W.A. Gerrard, B.C.H. Steele, Microstructural investigations on mixed RuO_2–TiO_2, J. Appl. Electrochem. 8 (1978) 417–425.
[10] M.T. Colomer, J.R. Jurado, Preparation and characterisation of gels of the ZrO_2–Y_2O_3–RuO_2 system, J. Non-Cryst. Solids 217 (1997) 48–54.
[11] E. Djurado, C. Roux, A. Hammou, Synthesis and structural characterisation of a new system: ZrO_2–Y_2O_3–RuO_2, J. Eur. Ceram. Soc. 16 (1996) 767–771.
[12] A. Hammou, E. Djurado, C. Roux, C. Micheau, Structural, thermal and electrical properties in the system: ZrO_2–Y_2O_3–RuO_2, Proc. Electrochem. Soc. 93 (1993) 48–58.
[13] Y.C. Long, Z.D. Zhang, K. Dwight, A. Wold, Preparation and characterisation of ZrO_2 stabilised with Ru(IV) and La (III), Mater. Res. Bull. 23 (1988) 631–636.
[14] M. Hrovat, S. Bernik, J. Holc, Subsolidus phase equilibria in the RuO_2–SrO–ZrO_2 system, J. Mater. Sci. Lett. 18 (1999) 1019–1020.
[15] T.P. Raming, W.E. van Zyl, H. Verweij, Chem. Mater. 13 (2001) 284–289.
[16] T.I. Panova, V. B Glushkova, M.G. Degen, E.P. Savchenko, Kinetics of grain growth in ZrO_2 based ceramics densified by explosive pressing, Inorg. Mater. 35 (1999) 233–236.
[17] D. Vrel, J.P. Petitet, X. Huang, T. Mashimo, Synthesis of ruthenium oxide high pressure phases by shock compaction, Phys. B 239 (1997) 9–12.
[18] E.P. Carton, Dynamic Compaction of Ceramics and Composites, Ph.D. Thesis, Delft University Press, Delft, The Netherlands, 1998.
[19] J.A.M. Bos, W.E. Vrielink, van der Linden, Non-destructive analysis of small irregularly shaped homogeneous samples by X-ray fluorescence spectrometry, Anal. Chim. Act. 412 (2000) 203–211.
[20] B. Tunaboylu, J.Mc. Kittrick, W.J. Nellis, S.R. Nutt, Dynamic compaction of Al_2O_3–ZrO_2 compositions, J. Am. Ceram. Soc. 77 (1994) 1605–1612.